

Brownian dynamics simulation of a polymer molecule in solution under elongational flow

U. S. Agarwal, Rohit Bhargava, and R. A. Mashelkar

Citation: *The Journal of Chemical Physics* **108**, 1610 (1998); doi: 10.1063/1.475531

View online: <http://dx.doi.org/10.1063/1.475531>

View Table of Contents: <http://scitation.aip.org/content/aip/journal/jcp/108/4?ver=pdfcov>

Published by the [AIP Publishing](#)

Articles you may be interested in

Brownian dynamics simulations of single polymer chains with and without self-entanglements in theta and good solvents under imposed flow fields

J. Rheol. **54**, 1061 (2010); 10.1122/1.3473925

Diffusion of Particle in Hyaluronan Solution, a Brownian Dynamics Simulation

AIP Conf. Proc. **708**, 263 (2004); 10.1063/1.1764135

Translational diffusion of polymer chains with excluded volume and hydrodynamic interactions by Brownian dynamics simulation

J. Chem. Phys. **118**, 8061 (2003); 10.1063/1.1564047

Brownian dynamics simulation of linear polymers under elongational flow: Bead-rod model with hydrodynamic interactions

J. Chem. Phys. **117**, 4030 (2002); 10.1063/1.1493187

Brownian dynamics of bead-rod-nugget-spring polymer chains with hydrodynamic interactions

J. Chem. Phys. **110**, 11608 (1999); 10.1063/1.479100



Brownian dynamics simulation of a polymer molecule in solution under elongational flow

U. S. Agarwal and Rohit Bhargava

Chemical Engineering Department, Indian Institute of Technology, Hauz Khas, New Delhi 110016, India

R. A. Mashelkar

Council of Scientific and Industrial Research, Anusandhan Bhavan, 2, Rafi Marg, New Delhi 110001, India

(Received 26 June 1997; accepted 16 October 1997)

We use Brownian dynamics simulation to study coil–stretch transition of macromolecules in solution. Into a simple elongational flow field, we introduce freely jointed bead-rod chain model molecules in their coiled and stretched states, and follow the conformational changes. We find good agreement of our simulation results with the available theoretical predictions for low and high strain rates ($\dot{\epsilon}$). At the intermediate elongation rates (near the onset of coil–stretch transition) of the flow field, we find that the residence time required for stretching of an initially coiled chain can be extremely large as compared to predicted $(1 + \ln(\sqrt{N}))\dot{\epsilon}^{-1}$, especially for the non-free-draining case. Hence, the chain conformation is dependent on the initial state of the chain molecule for residence time as long as $100\dot{\epsilon}^{-1}$. Thus, hysteresis is predicted when chain residence time in such an elongational flow field is limited, as in practical situations. Further, at such intermediate $\dot{\epsilon}$, the chain molecule is seen to undergo Brownian fluctuation induced jumps between a randomly coiled state and another partially stretched state. This suggests the existence of more than one equilibrium conformation that is unstable to Brownian fluctuations. © 1998 American Institute of Physics. [S0021-9606(98)51004-5]

I. INTRODUCTION

Small quantities of dissolved long chain polymers are used as additives to influence the rheology of liquids. Use of random coil polymers to enhance solution viscosity in weak flows is conventionally quantified in terms of intrinsic viscosity.^{1,2} Similarly, fully stretched polymer molecules have drawn interest in relation to chain scission behavior in strong flows.^{3–5} Further, many rheology modifying applications such as turbulent drag reduction and enhanced oil recovery are based on the flow induced stretching process of dissolved polymer coils, and the influence of the deformed polymer chains on solution rheology.^{1,2} In this paper we use Brownian dynamics simulation to examine the coil–stretch transition of polymers, and the hysteresis therein.

In the absence of any external forces, a polymer chain in solution remains coiled due to random Brownian motion. Under sufficiently strong flow conditions, the solvent drag force causes significant extension of the polymer molecule.^{1,6} For a given strain rate, there exists a certain level of stretching of a given macromolecule when the Brownian or elastic coiling forces are balanced by the stretching drag forces.^{7,8} The drag forces on an initially coiled macromolecule increase as it unravels, and it uncoils abruptly^{3,6,9} if the strain rate ($\dot{\epsilon}$) exceeds a critical value ($\dot{\epsilon}_{cs}$).

If an initially stretched chain is introduced into an elongational flow field, the outer segments experience a drag force greater than that experienced by a coiled chain introduced into the same flow field. This is due to the reduced hydrodynamic screening in the stretched state.⁹ This may lead to intermediate strain rates where a chain remains stretched if introduced into the flow field in its stretched state, and remains coiled if introduced in its coiled state. This

phenomenon of bistable equilibrium at a strain rate in the coil–stretch transition region was identified as the hysteresis by DeGennes,⁹ and its existence has been the subject of much theoretical debate,^{7,10–18} computer simulations,^{19,20} and experiments.^{21–24}

Early analyses of macromolecular stretching in extensional flow were based on dumbbell or bead-spring models,^{1,25–27} which have the inherent limitation in describing the stretching behavior due to their infinite extensibility.^{1,17,28,29} Rigid constraints were considered in dumbbell models³⁰ and bead-rod chains.^{20,29,31,32} Further, simplifying assumptions are often made, e.g., hydrodynamic interactions (HI) are neglected,^{26,31,32} or preaveraged values of the hydrodynamic interaction tensor have been used²⁷ in early analysis. Subsequently, finite extensibility of spring, and conformation dependent bead friction have been incorporated in analyzing elongational behavior of model dumbbells^{6,7–11} and chains.^{17,28,33–37} More recently, hydrodynamic interaction with higher order corrections has been incorporated.^{12,13,38}

Further, often theoretical predictions for chain conformation in elongational flow are available only for the steady state. However, this steady state is rarely achieved in practice as the residence time of a macromolecule in elongational flow is limited.¹⁸ Transient behavior during stretching has been analyzed by Brownian dynamics simulation of bead-spring chain models^{33,39} and bead-rod chain models,^{17,20,28,29,40} but these have concentrated primarily on the unraveling behavior of *initially coiled* chains. Only Dariinski and Saphiannikova¹⁹ used simulations of *dumbbell* model molecules for detecting hysteresis, and failed to find any, when the residence time was of the order of the macromo-

molecular relaxation time or greater. Thus, the question of hysteresis effect in coil-stretch transition of more realistic models, for limited residence times of practical interest, remains open. In this work we examine these issues by using Brownian dynamics simulations of isolated freely jointed bead-rod chains in solution under simple elongational flow field.

II. THEORY: FREELY JOINTED ("FLEXIBLE") BEAD-ROD CHAIN MODEL

A. Free-draining case (no HI)

Hassager³² analyzed the behavior of freely jointed bead-rod chain model macromolecules in elongational flows in the absence of hydrodynamic interaction. He obtained the following expressions for the solution elongational viscosity ($\bar{\eta} = (\tau_{xx} - \tau_{yy})/\dot{\epsilon}$),

$$\bar{\eta} - \bar{\eta}_s = (\bar{\eta}_\infty - \bar{\eta}_s) \left(1 - \frac{24kT}{N^2 \zeta l^2 \dot{\epsilon}} - \dots \right) \quad \text{at large } \dot{\epsilon}, \quad (1a)$$

$$\bar{\eta} - \bar{\eta}_s = (\bar{\eta}_0 - \bar{\eta}_s) \left(1 + \frac{N^2 \zeta l^2 \dot{\epsilon}}{90kT} + \dots \right) \quad \text{at small } \dot{\epsilon}, \quad (1b)$$

where $\bar{\eta}_s = 3\eta_s$ and η_s are the elongational and shear viscosities of the solvent alone, $\zeta = 6\pi\eta_s a$ is the bead friction factor, a is the bead radius, and l is the rod length. The asymptotic values of $\bar{\eta}$ at smallest $\dot{\epsilon}$ and at largest $\dot{\epsilon}$, for chains with large number of rods (N), are,

$$\bar{\eta}_0 - \bar{\eta}_s = n_0 \frac{\zeta l^2 N^2}{12} \quad (2a)$$

and

$$\bar{\eta}_\infty - \bar{\eta}_s = n_0 \frac{\zeta l^2 N^3}{12}, \quad (2b)$$

where $n_0 = cN_A/M$ is the number concentration of the polymer molecules, c is the mass concentration, and M the molecular weight of the polymer. N_A is the Avogadro number. Defining³⁶ the intrinsic viscosity (i.v.) as

$$[\bar{\eta}] = \lim_{c \rightarrow 0} \frac{\bar{\eta} - \bar{\eta}_s}{\bar{\eta}_s c}, \quad (3)$$

the corresponding expressions in terms of dimensionless quantities (represented by superscript *) are,

$$[\bar{\eta}]^* = [\bar{\eta}]_\infty^* \left(1 - \frac{24}{N^2 \dot{\epsilon}^*} - \dots \right) \quad \text{at large } \dot{\epsilon}^*, \quad (4a)$$

$$[\bar{\eta}]^* = [\bar{\eta}]_0^* \left(1 + \frac{N^2 \dot{\epsilon}^*}{90} + \dots \right) \quad \text{at small } \dot{\epsilon}^*, \quad (4b)$$

with the asymptotic values at smallest and largest $\dot{\epsilon}^*$ being

$$[\bar{\eta}]_0^*/a^* = \frac{\pi N^2}{6}, \quad (5a)$$

and

$$[\bar{\eta}]_\infty^*/a^* = \frac{\pi N^3}{6} = N[\bar{\eta}]_0^*/a^*. \quad (5b)$$

Here, $\dot{\epsilon}$ has been normalized by dividing by $kT/\zeta l^2$ (kT is the Boltzmann factor), and a by dividing by l , and $[\bar{\eta}]$ by multiplying with concentration $MN_A^{-1}l^{-3}$ (one polymer molecule per l^3 volume of the solution).

B. Non-free-draining case (with HI)

No analytical results are available for elongational behavior of non-free-draining bead-rod chains at arbitrary $\dot{\epsilon}$. However, the following available analytical results are applicable at asymptotic strain rates.

1. The unperturbed chain (approximation at $\dot{\epsilon} \rightarrow 0$)

Kirkwood and Riseman⁴¹ examined unperturbed linear flexible chain with hydrodynamic interaction described by Oseen,⁴² and obtained the following results for low shear flows,

$$[\eta]_0 = \frac{N_A \zeta N^2 l^2}{36 \eta_s M} F(X), \quad (6)$$

where $F(X)$ is a function² of $X = 2^{1/2}h$, with the hydrodynamic interaction parameter $h = \zeta N^{1/2}/(12\pi^3)^{1/2}\eta_s l$. Since at low or negligible deformation of polymer coil, $\bar{\eta} = 3\eta$, the corresponding dimensionless elongational intrinsic viscosity is obtained as

$$[\bar{\eta}]_0^*/a^* = \frac{\pi N^2}{6} F(X) \quad \text{with } X = (6/\pi)^{1/2} a^* N^{1/2}. \quad (7)$$

In the case of no hydrodynamic interaction, $X=0$, and $F(X)=1$, so that Eq. (5a) is recovered.

2. Multibead rod (approximation at $\dot{\epsilon} \rightarrow \infty$)

At the highest $\dot{\epsilon}$, a flexible bead-rod chain is completely stretched, and hence akin to a multibead rod. Bird *et al.*^{1,30} derived the following relations for multibead rods (with HI),

$$\bar{\eta} - \bar{\eta}_s = 3n_0 k T \lambda_N^{(2)} \times \left(\frac{1}{2} - \frac{3}{4X} + \frac{3}{4X} \frac{\exp(\pm X)}{\sqrt{X} \int_0^{\sqrt{X}} \exp(\pm y) dy} \right), \quad (8)$$

where $X = (9/2)\lambda_N^{(1)}\dot{\epsilon}$ and $\lambda_N^{(1)}$ and $\lambda_N^{(2)}$ are time constants given in Ref. 1. For $\dot{\epsilon} \rightarrow \infty$, this simplifies to

$$\bar{\eta}_\infty - \bar{\eta}_s = 6n_0 k T \lambda_N^{(2)}, \quad (9)$$

or,

$$[\bar{\eta}]_\infty^*/a^* = \pi \left(\sum_{\nu=-(N-1)}^{N-1} \nu \phi_\nu(2h', -\xi^2, N) \right), \quad (10)$$

where $h' = 0.75a^*$, $\xi = 2a^*$, and the function ϕ_ν is defined in Ref. 1. For the free-draining case ($h'=0$, $\phi_\nu = \nu/2$, and summation is over alternate ν), with large N , this reduces to Eq. (5b).

3. Fully stretched bead-rod chain (approximation at $\dot{\epsilon} \rightarrow \infty$)

Agarwal and Mashelkar⁴ presented a calculation for stresses in a non-free-draining bead-rod chain fully stretched

and aligned in a strong elongational flow field. Let us consider an N rod chain completely stretched and aligned along flow ($v_{xi} = \dot{\epsilon}x_i$, $\dot{\epsilon} \rightarrow \infty$) direction x , with its beads ($i = 1 \dots N + 1$) located at $x_i = (-Nl/2) + (i-1)l$. The component of the drag force \mathbf{F}_i^d along x is given as

$$F_{xi}^d = \zeta \left(v_{xi} + \frac{1}{kT} \sum_j \mathbf{D}_{xij}^0 \cdot \mathbf{F}_j^d \right), \quad (11)$$

where $v_{xi} = \dot{\epsilon}x_i$ is the unperturbed flow field. \mathbf{D}_{ij}^0 , the hydrodynamic interaction tensor between subunits i and j , is approximated by the modified Oseen tensor,⁴³

$$\begin{aligned} \mathbf{D}_{ij}^0 &= \frac{kT}{6\pi\eta_s a} \mathbf{I} \quad \text{for } i=j, \\ &= \frac{kT}{8\pi\eta_s r_{ij}} \left[\left(\mathbf{I} + \frac{\mathbf{r}_{ij}\mathbf{r}_{ij}}{r_{ij}^2} \right) + \frac{2a^2}{r_{ij}^2} \left(\frac{1}{3}\mathbf{I} - \frac{\mathbf{r}_{ij}\mathbf{r}_{ij}}{r_{ij}^2} \right) \right] \quad \text{for } i \neq j, \end{aligned} \quad (12)$$

where \mathbf{I} is the identity tensor and \mathbf{r}_{ij} is the displacement vector between beads i and j . Considering only the x component of drag force (neglecting the Brownian contribution at high $\dot{\epsilon}$),

$$F_{xi}^{d*} = x_i^* \dot{\epsilon}^* + \frac{3}{4}a^* \sum_{j \neq i} \left[\frac{2}{|j-i|} + 2(a^*)^2 \frac{2}{|j-i|^2} \left(-\frac{2}{3} \right) \right] F_{xj}^{d*}, \quad (13)$$

where x_i^* is position x_i made dimensionless by dividing by l , F_{xi}^{d*} represents the drag force F_{xi}^d made dimensionless by dividing by kT/l , and are evaluated by solution of this set ($i, j = 1 \dots N+1$) of coupled linear equations. The corresponding contribution to fluid stress and hence elongational viscosity can be calculated as

$$\bar{\eta}_\infty - \bar{\eta}_s = (n_0/\dot{\epsilon}) \sum_{i=1}^{N+1} \langle x_i^* F_{xi}^{d*} \rangle, \quad (14)$$

or,

$$[\bar{\eta}]_\infty^*/a^* = \frac{2\pi}{\dot{\epsilon}^*} \sum_{i=1}^{N+1} \langle x_i^* F_{xi}^{d*} \rangle. \quad (15)$$

III. BROWNIAN DYNAMICS SIMULATION

An isolated freely jointed bead-rod model chain consisting of $N = 100$ links and $(N+1)$ beads is used to analyze the behavior of a linear polymer molecule in a simple elongational flow field $\mathbf{v}(\mathbf{r})$ of strain rate ($\dot{\epsilon}$) given by

$$v_x = \dot{\epsilon}x, \quad v_y = -\frac{1}{2}\dot{\epsilon}y, \quad v_z = -\frac{1}{2}\dot{\epsilon}z.$$

Brownian dynamics simulation is carried out in steps of time Δt , in accordance with the SHAKE-HI algorithm.⁴⁴ During any step, the new position vector $\mathbf{r}_i(t + \Delta t)$ of the i th bead is calculated from the position $\mathbf{r}_i(t)$ at the beginning of the step by the relation

$$\mathbf{r}_i(t + \Delta t) = \mathbf{r}_i(t) + \frac{\Delta t}{kT} \sum_j \mathbf{D}_{ij}^0 \mathbf{F}_j^0 + \mathbf{R}_i(\Delta t), \quad (16)$$

where \mathbf{F}_j^0 is the sum of flow drag force (\mathbf{F}_j^d) and intramolecular (i.e., ‘‘bond’’ length constraint) forces acting on particle j at time t . The vector \mathbf{R}_i is the displacement of the particle due to Brownian motion, and has a Gaussian distribution with the following properties:

$$\langle \mathbf{R}_i \rangle = 0 \quad (17a)$$

and

$$\langle \mathbf{R}_i(t) \mathbf{R}_j(t + \Delta t) \rangle = 2\mathbf{D}_{ij}^0 \Delta t. \quad (17b)$$

IV. PARAMETERS

We follow chain extension during flow simulation by monitoring the square end-to-end distance (R_{ee}^2). R_{ee}^2 is normalized with respect to its mean random coil value (Nl^2). Thus, the value of normalized $R_{ee}^{2*} = R_{ee}^2/(Nl^2)$ varies from near 1 for a randomly coiled chain to $N=100$ for a fully stretched chain.

The contribution of the polymer to the elongational viscosity ($\bar{\eta} - \bar{\eta}_s$) is determined in terms of the intrinsic viscosity from the Kramers–Kirkwood relations,^{1,42}

$$[\bar{\eta}] = \frac{N_A}{\eta_s M \dot{\epsilon}} \sum_{i=1}^N \langle X_i T_{ix} - Z_i T_{iz} \rangle, \quad (18)$$

where X_i and Z_i are the x and z projections of the i th link, \mathbf{T}_i is the constraint force in the i th link, and is calculated using the Lagrangian constants obtained in the Allison and McCammon⁴⁴ algorithm. The corresponding normalized intrinsic viscosity is obtained as

$$[\bar{\eta}]^* = [\bar{\eta}] \frac{M}{N_A l^3} = \frac{2\pi a^*}{\dot{\epsilon}^*} \sum_{i=1}^{N+1} \langle X_i^* T_{ix}^* - Z_i^* T_{iz}^* \rangle, \quad (19)$$

where the projections X_i and Z_i are made dimensionless by dividing by l , the forces by kT/l , time by $\zeta l^2/kT$. Hereafter in the paper, only the dimensionless quantities are used, and the superscript $*$ is dropped for convenience.

V. SIMULATION METHODOLOGY

Computations are carried out for $N = 100$ rod chains. To study the contribution of hydrodynamic interaction to hysteresis in coil–stretch transition, two cases are considered:

- (1) free-draining case, i.e., no hydrodynamic interactions, and
- (2) non-free-draining case, i.e., with hydrodynamic interaction defined by ($a = 0.4$, or $h = 3.91$, or $h' = 0.3$).

Configuration development was followed during simulations carried out at various strain rates. The simulations were begun by starting with an *initially coiled* chain that was generated by successively joining 100 links. Each link was of length 1, and was randomly oriented. For each trajectory, a different initial random chain was generated, and a different set of Brownian contributions [\mathbf{R}_i in Eq. (16)] was selected. The trajectory simulation was carried out in small time steps of $\Delta t = 0.001$ or 0.002 , and use of a smaller time step did not affect typical simulation results. During the Brownian dy-

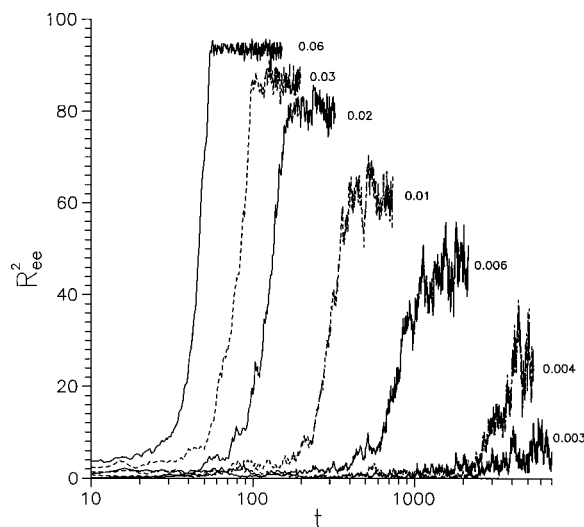


FIG. 1. Increase in R_{ee}^2 with time in elongational flow field of different strain rates ($\dot{\epsilon}$) shown in the figure, for stretching of free-draining, initially random coils.

namics simulation of a single chain, average values R_{ee}^2 and $[\eta]$ over each 1000 steps were stored as $R_{ee}^2(t)$ and $[\eta](t)$. These averages were plotted as separate points to study their evolution in time. Each trajectory simulation was continued until achieving flattening of $R_{ee}^2(t)$ and $[\eta](t)$ vs. t curves, to equilibrium values denoted $\langle R_{ee}^2 \rangle$ and $\langle [\eta] \rangle$, respectively. Such simulations were carried out for the *initially coiled* chains at different strain rates. Similar simulations at different strain rates were carried out also for chains *initially fully stretched* along the flow direction. Computations were carried out on a Silicon Graphics INDY IP 22 machine, and typical CPU time requirement per time step was 0.1 s.

VI. RESULTS AND DISCUSSIONS

A. Free-draining case (no HI)

Figure 1 shows the extension process of a free-draining initially coiled chain in extensional flow fields of various strain rates. Significant chain extension occurs only at strain rates $\dot{\epsilon}_{cs} \sim 0.003$ or greater. At $\dot{\epsilon} > 0.05$, near maximum possible stretching is achieved. Residence time t_f in a flow field required for stretching of a coiled chain decreases at higher strain rate (Fig. 1). t_f is determined as the time where the tangent to the transition part of the curves in Fig. 1 intersects the equilibrium value. For *affine* deformation, the Henky strain ($\epsilon_f = \dot{\epsilon} t_f$) required for complete stretching at high $\dot{\epsilon}$ is expected^{40,45} to be

$$\epsilon_f = 1 + \ln(\sqrt{N}) = 3.3 \quad \text{for } N = 100. \quad (20)$$

For the free-draining case, we find ϵ_f to be about 2.9–3.5 at $\dot{\epsilon} \sim 0.01$ or higher (Fig. 2): indicating *affine* deformation at these $\dot{\epsilon}$. However, we note that based on simulations of Ralison and Hinch²⁸ and van der Brule,³³ James and Sridhar⁴⁵ had estimated ($\epsilon_f \sim 6.5$). Figure 3 shows the relaxation of initially stretched chains introduced into elongational flow fields of various $\dot{\epsilon}$. At $\dot{\epsilon} \geq 0.06$, the chain remains stretched,

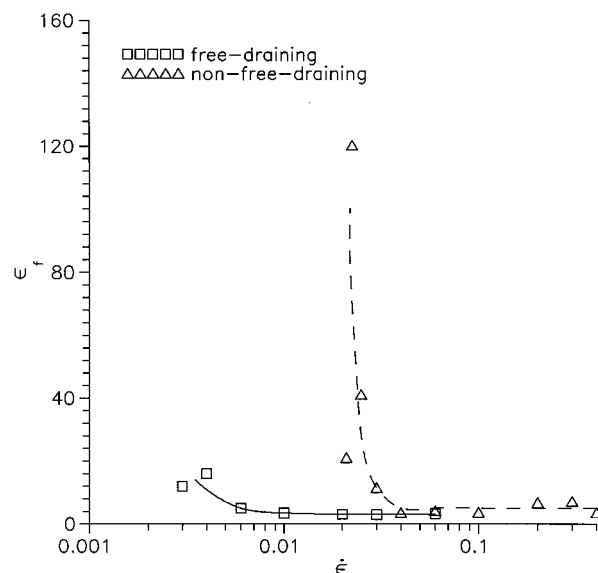


FIG. 2. $\epsilon_f = \dot{\epsilon} t_f$ for stretching of initially random coiled chains to near equilibrium in flow fields of different $\dot{\epsilon}$.

while at $\dot{\epsilon} \leq 0.002$, complete relaxation takes place. At intermediate strain rates, the relaxation is partial. Starting from a fully stretched state, the time required for relaxation in the absence of flow is $\tau \sim 600$ (Fig. 3, $\dot{\epsilon} = 0$), which suggests^{46,47} $\dot{\epsilon}_{cs}$ for stretching as greater than $\tau^{-1} \sim 0.0016$, in agreement with results of Fig. 1 and Fig. 3. In Fig. 4, we examine the equilibrium stretching results for free-draining chains introduced into the flow fields initially in their coiled and stretched states. At all strain rates, we see no dependence of $\langle R_{ee}^2 \rangle$ on the initial state of the chain. We again notice the coil–stretch transition at $\dot{\epsilon}_{cs} \sim 0.003$ or greater. The corresponding steady state $[\eta]/a$ from our simulations is presented in Fig. 5, along with Hassager's predictions (Sec. II A). We find an excellent agreement at high $\dot{\epsilon}$. In the in-

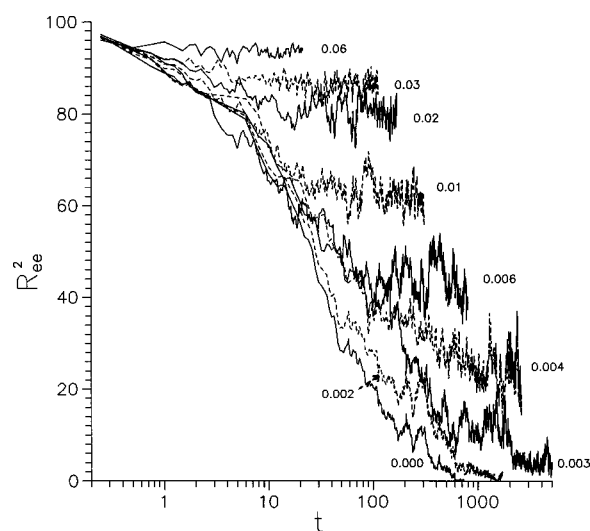


FIG. 3. Decrease in R_{ee}^2 with time in elongation flow field of different strain rates ($\dot{\epsilon}$) shown in the figure, for coiling of free-draining, initially fully stretched chain.

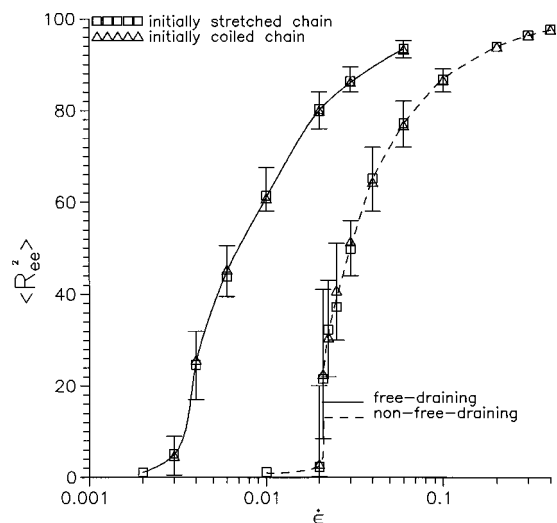


FIG. 4. Equilibrium mean square end-to-end distance at different strain rates, for free-draining (—) and non-free-draining (---) chains. The data points are the average values, and the bars show the range of fluctuations.

intermediate range, Eq. (4a) overpredicts, and Eq. (4b) underpredicts, as expected due to the truncations in these equations. At $\dot{\epsilon} \leq 0.002$, the fluctuating contribution of the Brownian forces is predominant (as compared to drag forces), and statistically reliable averages could not be obtained.

B. Non-free-draining case (with HI, $a=0.4$)

The uncoiling process of non-free-draining initially coiled chains in flow fields of different $\dot{\epsilon}$ are shown in Fig. 6, and the coiling process of initially fully stretched chains is shown in Fig. 7. We notice that significant stretching of coiled chains occurs at $\dot{\epsilon} \sim 0.0225$ or greater, and complete relaxation of fully stretched chains occurs at $\dot{\epsilon} \leq 0.01$. In Fig. 8 we show the uncoiling and coiling processes at some in-

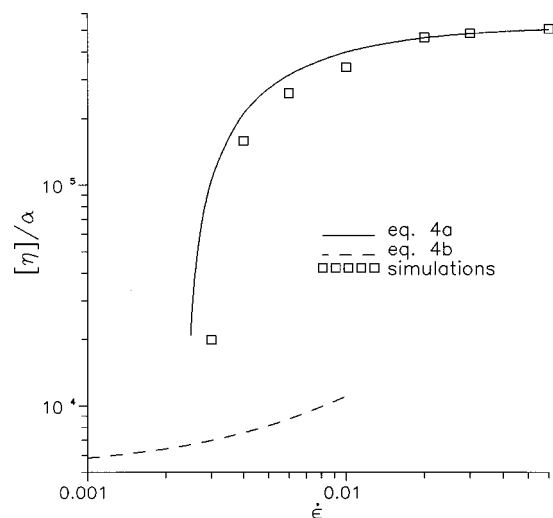


FIG. 5. Equilibrium intrinsic viscosity at different strain rates, for free-draining chains. The simulation results are compared with Hassager's (Ref. 32) theoretical predictions at high and low $\dot{\epsilon}$ range.

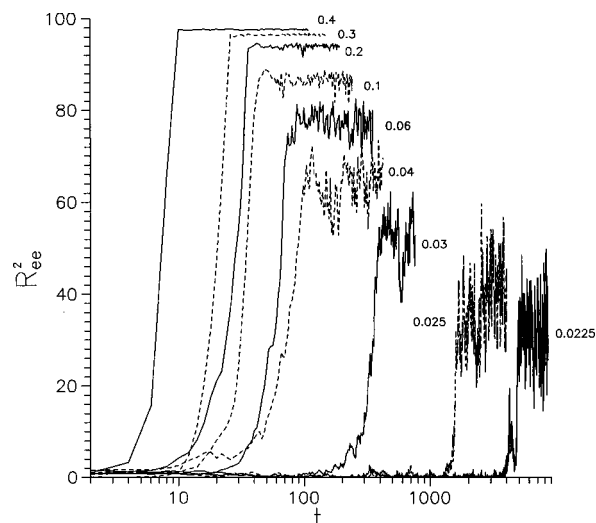


FIG. 6. Increase in R_{ee}^2 with time in elongation flow field of different strain rates ($\dot{\epsilon}$) shown in figure, for stretching of non-free-draining, initially random coiled chain.

termediate strain rates. Figure 2 shows the total Hencky strain $\epsilon_f = \dot{\epsilon} t_f$ required for initially coiled non-free-draining chains to achieve their equilibrium conformation at various $\dot{\epsilon}$. At $\dot{\epsilon} \geq 0.04$, ϵ_f values are found to be 3.5 to 6.5. These higher values for the non-free-draining case indicate somewhat slower than *affine* deformation here. This is because in the present HI case, the inner beads of initially coiled chains are efficiently shielded from the drag of bulk fluid flow. At intermediate strain rates near $\dot{\epsilon} = 0.02$, the chain deformation is extremely slow (as compared to $t_f \sim \dot{\epsilon}^{-1}$, or $\epsilon_f = \text{constant}$ at higher $\dot{\epsilon}$, see Fig. 2). Fuller and Leal,⁷ and Leal,⁸ also predicted such delayed approach to equilibrium for dumbbells at intermediate $\dot{\epsilon}$. This is because here the fluid drag is sufficient to maintain a preexisting extended state, but the beginning of stretching of a random coil is made possible only by

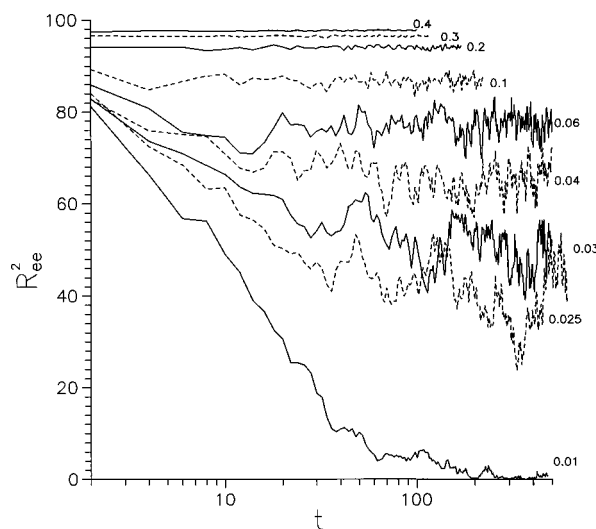


FIG. 7. Decrease in R_{ee}^2 with time in elongation flow field of different strain rates ($\dot{\epsilon}$) shown in the figure, for coiling of non-free-draining, initially fully stretched chain.

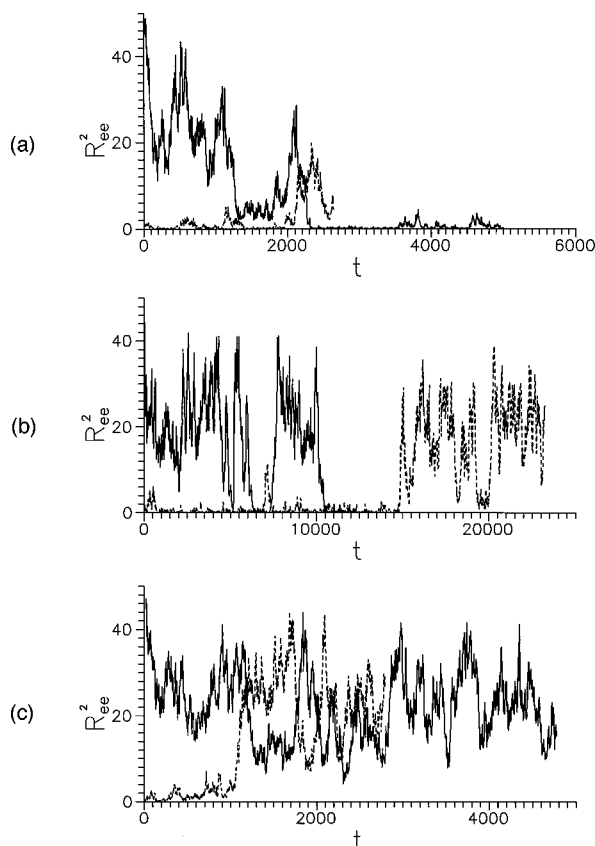


FIG. 8. Conformation changes of non-free-draining chains with time in elongational flow field of strain rates (a) 0.02, (b) 0.0204, and (c) 0.021. Initially random coiled chains (---) and initially fully stretched chains (—).

Brownian diffusion induced coil expansion leading to reduction in hydrodynamic shielding. Hence, the observed ϵ_f at these intermediate $\dot{\epsilon}$ is strongly dependent on the initial chain conformation which, being random, could be expanded to different extents. Thus, dependence of single trajectory ϵ_f on $\dot{\epsilon}$ may be irregular, particularly near onset $\dot{\epsilon} = 0.02$ (Fig. 2). However, the key feature of very high ϵ_f at these intermediate $\dot{\epsilon} \sim \dot{\epsilon}_{cs}$ is consistent.

Thus, in these intermediate $\dot{\epsilon}$ elongational flow fields experienced for a limited time (often the case in practical situations^{18,45,47}), an initially stretched molecule may remain significantly stretched, while an initially coiled molecule may not have yet begun to uncoil. Thus, the extent of macromolecular stretching (or solution viscosity) is expected to be a function of the initial state (coiled or stretched) and hence the “history” of the macromolecules. In other words, hysteresis is predicted. This dependence of elongational viscosity on history, as also observed in experiments,^{21–23} reflects that its measurement will depend on the apparatus used. The search for an appropriate elongational viscometer thus continues.^{45,48} Further, as concluded from our Fig. 2, the Eq. (20) for estimation of strain required for unfolding of a randomly coiled chain is clearly suspect at the intermediate strain rates, and serves only as lower bound. Hunkeler *et al.*⁴⁷ recently found ϵ_f values for polystyrene to be be-

TABLE I. Intrinsic viscosity in the presence of HI ($a = 0.4$).

Theoretical			Simulation	
$\dot{\epsilon}$	$[\eta]/a$		$\dot{\epsilon}$	$[\eta]/a$
0	830	[Eq. (7)]	0.01	808
∞	1.30×10^5	[Eqs. (10), (15)]	0.4	1.27×10^5

tween 4 and 15, depending on the solvent quality. Considering the above discussed dependence of ϵ_f on initial coil conformation, and the known effect of solvent quality on the coil size in quiescent solution, a solvent dependent ϵ_f was thus to be expected.

In Table I we present the equilibrium $[\eta]/a$ results from our simulations at the smallest and the highest $\dot{\epsilon}$, and compare these with the corresponding theoretical predictions [Eq. (7) and Eqs. (10) or (15), respectively], when a good agreement is seen. As seen from Figs. 6–8, the equilibrium chain conformation, as indicated by $\langle R_{ee}^2 \rangle$, is independent of the initial state of the chain molecule. These equilibrium results for the non-free-draining case are presented in Fig. 4, and we again notice the onset of coil–stretch transition near $\dot{\epsilon} \sim 0.02$.

The chain coiling–uncoiling behavior at strain rates near this onset ($\dot{\epsilon} \sim 0.02$) is very interesting [Figs. 8(a)–8(c)]. We notice that the chain conformation does not approach a single equilibrium, and instead it oscillates significantly in a range of extension. For example, at $\dot{\epsilon} = 0.02$ [Fig. 8(a)], we see that following the initial coiling (relaxation) period, the chain seems to spend *most of its time in a coiled state*. At $\dot{\epsilon} = 0.0204$ [Fig. 8(b)], the chain seems to spend comparable amounts of time in a randomly coiled state ($\langle R_{ee}^2 \rangle \sim 0–6$) and a partially stretched state ($\langle R_{ee}^2 \rangle \sim 10–40$), with *occasional jumps* between these states. At $\dot{\epsilon} = 0.021$, [Fig. 8(c)], the chain *continuously fluctuates*, though staying all the time (following the initial uncoiling) in a partially extended state ($\langle R_{ee}^2 \rangle \sim 4–40$). This behavior at long residence time in flow at intermediate $\dot{\epsilon}$ also is independent of the initial state of the chain. Though fluctuations are present at all $\dot{\epsilon}$ (Figs. 6–8), the fluctuations increase as the $\dot{\epsilon}$ decreases to the transition onset value $\dot{\epsilon} \sim 0.02$.

For the initially coiled molecule during the simulation at $\dot{\epsilon} = 0.0204$ shown in Figs. 8(b), Fig. 9 shows typical snapshots in random coil state (at $t = 11\,222$) and in partially

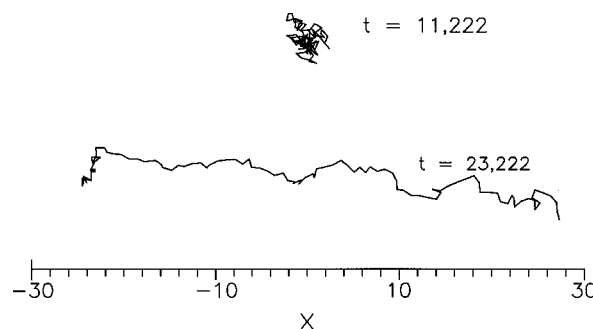


FIG. 9. Snapshots of XY projection of the non-free-draining, initially coiled chain in $\dot{\epsilon} = 0.0204$ flow at two different times.

stretched state (at $t = 23\,222$). As seen in Fig. 8(b), the transition between such conformational states is sudden and reversible. We refer to these as jumps since the time taken during the movement between these two states is much shorter than the time spent in each of these states. These jumps seem to be caused by Brownian motion caused fluctuations in coil size that also cause fluctuations in hydrodynamic drag.^{12,49} For example, when in a random coil equilibrium conformation at a given $\dot{\epsilon}$, a certain Brownian fluctuation could expand the coil size, thereby increasing the hydrodynamic drag sufficiently to stretch the chain to another local equilibrium (a partially extended conformation). Similarly, another sufficiently strong fluctuation reducing the coil size could lead the chain back to the random coil state. Magda *et al.*¹² had many years back realized the importance of these fluctuations near critical strain rates.

Thus, we seem to have some evidence of two equilibrium states of macromolecular coil in the intermediate $\dot{\epsilon}$ region. However, the macromolecule jumps between these unstable states over sufficient residence time, due to Brownian fluctuations. These jump effects may be present in individual macromolecules in elongational flows with long residence time at stagnation points. However, as measurements like viscosity, birefringence, or light scattering involve averaging over many macromolecules (perhaps in different states of stretching), such time dependent jumps are not expected to be observed in these measurements. Experimental observation of this effect would require examination of stretching of a single macromolecule with time, which may become possible using techniques like that employed by Perkins *et al.*⁵⁰

For steady flows, Pincus⁵¹ had proposed a dynamic blob model for partially stretched macromolecules. Our partially stretched chain shown in Fig. 9 has some similarity to this. Preference for higher extension at the centers than at the ends, proposed in recent models,^{49,52,53} is only marginal. But this could be related to the limited segments employed in our chain model. Many recent investigations of polymer conformations in elongational flows reported observation of folds, back loops, hairpin or kinks like intramolecular structures,^{17,20,28,29,31,33,40,45,47} that undulate very slowly. But these were primarily related to transient flows that were very strong (Brownian motion was even neglected in some of these), so that the chain molecules froze in partially extended conformations. We noticed no such back loops in our simulations for long residence times. We believe that since the strain rates considered here are not extremely high, the Brownian motion is sufficient to facilitate removal of such unstable back loops, if any.

VII. CONCLUSIONS

Results are presented for Brownian dynamics simulation of conformational changes of bead-rod chain model macromolecules introduced into a simple elongation flow field. When the hydrodynamic interaction is considered, we find that the response time for stretching of a coiled chain can be two orders of magnitude larger than ϵ^{-1} at the intermediate elongation rates $\dot{\epsilon}$ (near the onset of coil–stretch transition).

Hence, hysteresis would be observed at intermediate $\dot{\epsilon}$ if the time of observation is limited. Further, we find that during long time simulations at these $\dot{\epsilon}$, the conformation of a non-free-draining chain molecule may undergo sudden reversible jumps between “randomly coiled” and “partially stretched” states. This suggests existence of more than one unstable equilibrium conformation. This phenomenon is not observed during simulations in the absence of hydrodynamic interactions, and is perhaps induced by fluctuations in HI due to Brownian motion induced conformational changes.

ACKNOWLEDGMENTS

Financial support provided through Grant No. III.4(18)/93-ET from the Department of Science and Technology is gratefully acknowledged.

- ¹R. B. Bird, C. F. Curtiss, R. C. Armstrong, and O. Hassager, *Dynamics of Polymeric Fluids, Vol. 2 of Kinetic Theory* (Wiley, New York, 1987).
- ²H. Yamakawa, *Modern Theory of Polymer Solutions* (Harper and Row, New York, 1971).
- ³J. A. Odell and A. Keller, *J. Polym. Sci., Polym. Phys. Ed.* **24**, 1889 (1986).
- ⁴U. S. Agarwal and R. A. Mashelkar, *J. Chem. Phys.* **100**, 6055 (1994).
- ⁵U. S. Agarwal and R. A. Mashelkar, *J. Non-Newtonian Fluid Mech.* **54**, 1 (1994).
- ⁶A. Peterlin, *Pure Appl. Chem.* **12**, 563 (1966).
- ⁷G. G. Fuller and L. G. Leal, *Rheo Acta* **19**, 580 (1980).
- ⁸L. G. Leal, in *Polymer Flow Interactions*, edited by Y. Rabin (AIP, New York, 1985).
- ⁹P. G. DeGennes, *J. Chem. Phys.* **60**, 5030 (1974).
- ¹⁰E. J. Hinch, *Proc. Symp. Polym. Lubrification*, Brest (1974).
- ¹¹R. I. Tanner, *Trans. Soc. Rheol.* **19**, 557 (1975).
- ¹²J. J. Magda, R. G. Larson, and M. E. Mackay, *J. Chem. Phys.* **89**, 2504 (1988).
- ¹³P. Biller, H. C. Ottinger, and F. Petruccione, *J. Chem. Phys.* **85**, 1672 (1986).
- ¹⁴X. Fan and R. B. Bird, *J. Non-Newtonian Fluid Mech.* **18**, 255 (1985).
- ¹⁵F. S. Heyney and Y. Rabin, *J. Chem. Phys.* **82**, 4362 (1985).
- ¹⁶M. L. Mansfield, *J. Chem. Phys.* **88**, 6570 (1988).
- ¹⁷J. M. Wiest, L. E. Wedgewood, and R. B. Bird, *J. Chem. Phys.* **90**, 586 (1989).
- ¹⁸Y. Rabin, F. S. Henyey, and R. K. Pathria, in *Polymer Flow Interactions*, edited by Y. Rabin (AIP, New York, 1985).
- ¹⁹A. A. Darinskii and M. G. Saphiannikova, *J. Non-Cryst. Solids* **172–174**, 932 (1994).
- ²⁰T. W. Liu, *J. Chem. Phys.* **90**, 5826 (1989).
- ²¹D. F. James, B. D. McLean, and J. H. Saringer, *J. Rheol.* **31**, 453 (1987).
- ²²A. M. Wunderlich and D. F. James, *Rheol. Acta* **26**, 522 (1987).
- ²³K. Vissmann and H.-W. Bewersdorff, *J. Non-Newtonian Fluid Mech.* **34**, 289 (1990).
- ²⁴J. A. Odell, A. Keller, and A. J. Muller, in *Polymers in Aqueous Media*, edited by J. E. Glass (ACS, Washington 1989), Chap. 11.
- ²⁵W. Kuhn, *Kolloid-Z.* **68**, 2 (1934).
- ²⁶P. E. Rouse, *J. Chem. Phys.* **21**, 1272 (1953).
- ²⁷B. H. Zimm, *J. Chem. Phys.* **24**, 269 (1956).
- ²⁸J. M. Rallison and E. J. Hinch, *J. Non-Newtonian Fluid Mech.* **29**, 37 (1988).
- ²⁹E. J. Hinch, *J. Non-Newtonian Fluid Mech.* **54**, 209 (1994).
- ³⁰R. B. Bird, M. W. Johnson, and J. F. Stevenson, in *Proceedings of the 5th International Congress on Rheology*, Vol. 4, edited by S. Onogi (University of Tokyo Press, Tokyo, 1970).
- ³¹D. Acierno, G. Titomantio, and G. Marrucci, *J. Polym. Sci., Polym. Phys. Ed.* **12**, 2177 (1974).
- ³²O. Hassager, *J. Chem. Phys.* **60**, 2111 (1974).
- ³³B. H. A. A. van den Brule, *J. Non-Newtonian Fluid Mech.* **47**, 357 (1993).
- ³⁴M. L. Mansfield and L. Rakesh, *Polym. Commun.* **30**, 327 (1989).
- ³⁵J. M. Kobe and J. M. Wiest, *J. Rheol.* **37**, 947 (1993).
- ³⁶W. Carl and W. Bruns, *Macromol. Theory Simul.* **3**, 295 (1994).
- ³⁷J. M. Wiest and R. I. Tanner, *J. Rheol.* **33**, 281 (1989).

- ³⁸J. J. Lopez Cascales, F. G. Diaz, and J. Garcia de la Torre, *Polymer* **36**, 345 (1995).
- ³⁹K. D. Knudsen, J. G. Hernandez Cifre, J. J. Lopez Cascales, and J. Garcia de la Torre, *Macromolecules* **28**, 4660 (1995).
- ⁴⁰R. G. Larson, *Rheol. Acta* **29**, 371 (1990).
- ⁴¹J. G. Kirkwood and J. Riseman, *J. Chem. Phys.* **14**, 415 (1948).
- ⁴²C. W. Oseen, *Hydrodynamik* (Akademische Verlagsgesellschaft, Leipzig, 1927).
- ⁴³J. Rotne and S. Prager, *J. Chem. Phys.* **50**, 4831 (1969).
- ⁴⁴S. A. Allison and J. A. McCammon, *Biopolymers* **23**, 167 (1984).
- ⁴⁵D. F. James and T. Sridhar, *J. Rheol.* **39**, 713 (1995).
- ⁴⁶G. Marrucci, *Polym. Eng. Sci.* **15**, 229 (1975).
- ⁴⁷D. Hunkeler, T. Q. Nguyen, H. H. Kausch, *Polymer* **37**, 4257 and 4271 (1996).
- ⁴⁸R. Kroger and H. J. Rath, *J. Non-Newtonian Fluid Mech.* **57**, 137 (1995).
- ⁴⁹R. G. Larson and J. J. Magda, *Macromolecules* **22**, 3004 (1989).
- ⁵⁰T. T. Perkins, D. E. Smith, R. G. Larson, and S. Chu, *Science* **268**, 83 (1995).
- ⁵¹P. Pincus, *Macromolecules* **10**, 210 (1977).
- ⁵²G. Ryskin, *J. Fluid Mech.* **178**, 423 (1987).
- ⁵³Y. Rabin, *J. Chem. Phys.* **88**, 4014 (1988).